The link between a heterogeneous model and its flow response: examples from fault damage zones highlighting issues in domain discretization and flow simulation

J. MA[1], A. Z. VASZI[2], G. D. COUPLES[1] & S. D. HARRIS[2]

[1]*Institute of Petroleum Engineering, Heriot-Watt University, Edinburgh EH14 4AS, UK (e-mail: Jingsheng.Ma@pet.hw.ac.uk)*

[2]*Rock Deformation Research Ltd, School of Earth and Environment, University of Leeds, Leeds LS2 9JT, UK*

Abstract: Natural fault damage zones (FDZs) are characterized by complex geometries and topologies, and by strongly-contrasting material properties. Accurate simulation of fluid flow in such systems is dependent on the method of discretization and the mathematical representation of the flow. In this paper, we focus on the conceptual and methodological issues that link a model of a heterogeneous system and its flow response. We study FDZs as our example, where each thin fault strand is a barrier to flow. We examine two contrasting discretization schemes and apply them to 2D FDZ models that contain a realistic array of linear fault traces. Both schemes produce results that are generally in good agreement, and agree with the results calculated by a more accurate (but computationally less efficient) reference scheme. However, differences occur when the discretization approach fails to maintain the fault connectivity (topology) of the input model. It is important to guide the modelling by identifying any continuous flow pathways in the matrix linking fluid inlets and outlets (Through-Going Regions, TGRs). We illustrate a new scheme that identifies all TGRs and determines a grid that is just fine enough to resolve them.

Natural fault damage zones (FDZs) commonly contain many small faults that are thin compared to their lateral extents. The small faults form complex arrays that play a significant role in governing fluid flow within or across the entire FDZ. To predict the net flow effects of the complete system (i.e. at a coarse scale), the components of the FDZ must be idealized to create a model, and that model must then be used as an input for flow simulation leading to an upscaled flow property (see Harris *et al.* 2007 for a review). Although there are a number of issues that must be considered in the modelling of FDZs, including the choice of sampling scales and positions within the FDZ, and the choice of the scale of faults to be modelled, this paper is concerned with other issues related to the choices that must be made in terms of how to represent the architecture and properties of the FDZ components within the fine-scale models numerically. Specifically, we examine how aspects of the representation approach may impact the simulation output and thus the prediction of larger-scale flow effects.

Fault zones commonly consist of an inner fault core zone, accommodating most of the displacement, surrounded by a complex zone of deformation, called the damage zone, extending from distances of perhaps metres to tens of metres on either side of the core zone (Chester & Logan 1986; Cowie & Scholz 1992; Caine & Forster 1999). The damage zone typically exhibits subseismic-scale, low-throw, thin faults, which are typically less than a few millimetres in thickness and which, although constituting only a small fraction of the volume of the whole zone, can provide significant additional retardation to fluid flow in combination with the flow retardation of the core zone (Knipe *et al.* 1998; Harris *et al.* 2007). In siliciclastic sedimentary rocks, these small faults may take the form of deformation bands that act as partial barriers to fluid flow (e.g. Knipe *et al.* 1998; Manzocchi *et al.* 1998; Shipton & Cowie 2001; Jourde *et al.* 2002; Odling *et al.* 2004; Harris *et al.* 2007). Several deformation mechanisms and processes, including cataclasis, and clay smearing and diagenesis, can result in potentially significant reduction in the permeability of conventional deformation bands in sandstones by several orders of magnitude relative to the host sedimentary rock (Knipe *et al.* 1998). These deformation bands may or may not be accompanied by open fractures which could enhance the bulk permeability (e.g. Jourde *et al.* 2002). In this paper, we are only concerned with fault damage zones where thin fault strands act as partial barriers/baffles to flow (we do not address any effects associated with open fractures).

The geometrical and topological characteristics of the thin fault strands, along with their poro-perm

From: JOLLEY, S. J., BARR, D., WALSH, J. J. & KNIPE, R. J. (eds) *Structurally Complex Reservoirs.* Geological Society, London, Special Publications, **292**, 337–352.
DOI: 10.1144/SP292.19 0305-8719/07/$15.00

properties (in relation to the matrix properties), are the important factors that determine the net flow response of the whole FDZ. However, the physical dimensions of thin faults in FDZs mean that they are too small to be detectable individually on even the best seismic data, and other sampling methods (such as those used in wellbores) do not provide full spatial coverage. Thus, models of FDZs have to be developed using limited hard and soft data, with the attendant issues as to the accuracy or representivity of any model. Certain characteristics of the fault arrays can be obtained from well core, core plug and well logs, for example allowing a determination of fault orientations, and their terminations and crossings, that play an important role in determining fault connectivity (Manzocchi *et al.* 1998; Harris *et al.* 2003). Soft data is often obtained from outcrop analogues or from geomechanical methods (including numerical simulations or laboratory analogues). Outcrop information provides an opportunity to observe patterns and inter-relationships (such as clustering), and enables process models to be defined (Gillespie *et al.* 1993). Geomechanical simulations can provide additional insights into the evolution of fault systems and their localized strain–stress fields to enable the model-based predictions of small fault density and orientation distributions (Bourne & Willemse 2001; Maerten *et al.* 2006; Lewis *et al.* 2004, 2007; Couples 2005; Schopfer *et al.* 2006; Couples *et al.* 2007). It may be the case that at the present state of that specialty, metre- or larger-scale geomechanical models may have greater predictive power than do sub-metre-scale models (because at the larger scale, the predicted deformation features will be represented as bodies, albeit thin ones, of porous material, whereas at the sub-metre scale, the simulation outcomes represent deformation types that need to be treated as discrete features). Realistic FDZ models may be generated stochastically using information derived from such hard and soft data (Harris *et al.* 2003).

The physical dimensions of the many thin faults in FDZs make it difficult to discretize the spatial domains of FDZ models, and the flow equations related to those domains. It is often impractical to discretize thin, but typically irregular (in geometry) faults explicitly and precisely because this approach generates grids or meshes that contain too many cells, making it difficult to solve the flow equations efficiently. Because FDZ models of necessity must be stochastic, many individual models need to be created, and each one taken to flow simulation, to produce bulk flow characteristics that vary as a function of the stochastic parameters. Thus, efficiency in model creation and in flow simulation, is an essential consideration.

Two types of discretization schemes for fault arrays have recently been developed: one by Odling *et al.* (2004) and Vaszi *et al.* (2004); and one by Ma *et al.* (2006). These two schemes represent different approaches to fault discretization and flow simulation, and both can be shown (see below) to produce accurate results when the discretization maintains the model fault connectivity. Maintaining the connectivity becomes more important when the matrix permeability is over two orders of magnitude greater than that of faults (Manzocchi *et al.* 1998; Walsh *et al.* 1998*a*, *b*; also see the results in this paper). In heterogeneous systems like those considered here, a significant problem with model discretization is to capture the critical fault connectivity without consequently inducing alterations to the connectivity of a matrix region. A matrix region that connects from the flow inlets to the flow outlets is referred to as a Through-Going Region (TGR), introduced in the work by Ma & Couples (2007). TGRs could influence fluid flow significantly if the fluid is forced to flow through them as the only available pathway. One of the possible settings, relevant to this work, is that the permeability contrast between the faults and matrix is high, and the TGR is not very tortuous (and thus plays an important role in the flow process). When a TGR is a flow-influential pathway, it is important to prevent it from being mis-discretized into a non-TGR.

The potential impact of these discretization errors, relative to the reliability and robustness of the flow solution, requires answers to two questions. Where do the errors typically occur? What are their impacts? A sensitivity analysis is one of the classical approaches to solving this problem. Step-wise refined grids are constructed, and the solution is calculated for each grid. Any sudden change of the solution, from one grid resolution to the next, indicates the insufficiency of the grid corresponding to the former resolution. However, this approach has two important limitations. First, for a FDZ model, it is difficult to know that any particular grid resolves all flow-influential TGRs. Second, this approach is computationally expensive because a full flow solution must be obtained for each grid resolution.

Ma & Couples (2007) describe a new and efficient alternative approach that addresses these two questions without incurring either of the difficulties noted above. Based on hierarchical domain decomposition, morphological analysis of objects and network flow modelling, that scheme is capable of identifying the existence of TGRs and, if they exist, the most flow-influential TGRs for a given FDZ model. Therefore, the scheme can determine a grid, called a guiding grid, which is sufficient to resolve the flow-influential TGRs. This guiding grid can then be used to constrain fault

simplification in the subsequent construction of structured or unstructured grids for simulations. Consequently, simulated solutions on such grids will no longer be subject to the type of discretization errors that are the focus of this paper.

This paper makes a comparison of the two discretization schemes (using 2D examples for simplicity and clarity) and considers the role of the guiding-grid scheme in reducing the discretization errors associated with the mis-representation of fault connectivity. For some FDZ model configurations, and some flow regimes, the concerns over discretization errors prove to be irrelevant, and both approaches yield good results. However, some model configurations reveal the existence of artefacts due to the discretization approach. For the single-phase flow considered in this work, the latter case is likely to be associated with a high permeability contrast between fault and matrix and where there is low flow tortuousity in the FDZ (see Walsh *et al.* 1998*a*, *b* for a further discussion). In order to account for these effects in the final analysis of uncertainty, it is essential to have a solid understanding of the link between a model and the calculated flow through that model.

Comparison of discretization schemes for FDZs

The two discretization schemes to be compared are that of Odling *et al.* (2004) and Vaszi *et al.* (2004) in 2D, and that of Ma *et al.* (2006). Both schemes were developed to enable permeability upscaling in FDZs by solving flow equations across model domains comprising stochastic realizations of arrays of thin fault strands. Here we consider only single-phase flow to reduce the number of parameters and thus enable us to focus attention on the key issue of the role of discretization. When a single-phase fluid is incompressible and flows in a steady state condition, the flow equations (without gravity and source/sink terms) read as follows:

$$\begin{cases} \nabla \cdot \boldsymbol{v} = 0 \\ \boldsymbol{v} = -\boldsymbol{k}\nabla p \end{cases} \text{ on } \Omega, \tag{1}$$

where Ω is the domain of the problem, $\boldsymbol{v}$ is the Darcy velocity (flux rate across a unit area), p is the fluid pressure, and $\boldsymbol{k} = \boldsymbol{k}_{\text{abs}}/\mu$, where $\boldsymbol{k}_{\text{abs}}$ is the absolute permeability tensor of the medium and μ is the fluid viscosity.

DFFM

The discretization scheme of Odling *et al.* (2004) and Vaszi *et al.* (2004) is based on the Control-Volume Finite-Difference method implemented on a structured grid. This scheme is referred to as the Discrete Fault Flow Model (DFFM). Instead of trying to model faults directly, DFFM requires a fine structured grid to be defined on which the flow impact of the faults is accounted for by modifying the transmissibility between control-volumes according to the occurrence of faults, and their individual properties and geometries (Fig. 1). A control volume of DFFM is defined around each grid cell node (see Fig. 1a). This scheme uses a staggered grid arrangement where fluxes, $\boldsymbol{q}$, are associated with the midpoints of control volume edges, and pressures, $\boldsymbol{p}$, at the grid cell nodes (see Fig. 1b). Permeability is defined on a different grid in which a cell is centred at a midpoint of a control volume facet (see Fig. 1c).

The flow equations (Equation 1) are then discretized on each control volume to conserve mass (i.e. Equation 2a). Fluxes are related to nodal pressures

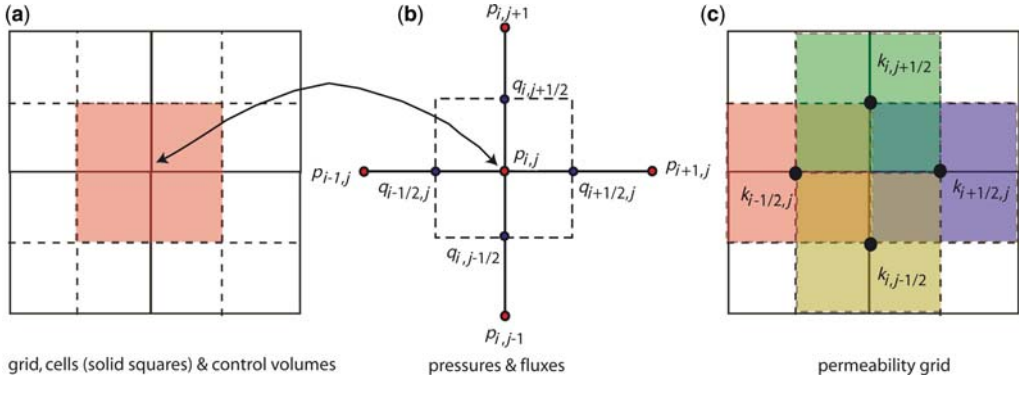

Fig. 1. Illustration of DFFM control volume finite difference scheme. (**a**) grid cells (divided by solid lines) and control volumes (divided by dotted lines); (**b**) discrete pressures (red) and fluxes (blue); (**c**) permeability grid.

via Darcy's law along each grid canonical direction as shown in Equations 2b to 2c.

$$(q_{i+1/2,j} - q_{i-1/2,j}) + (q_{i,j+1/2} - q_{i,j-1/2}) = 0 \quad (2a)$$

$$q_{i\pm1/2,j} = \mp T_{i\pm1/2,j}(p_{i\pm1,j} - p_{i,j}) \quad (2b)$$

$$q_{i,j\pm1/2} = \mp T_{i,j\pm1/2}(p_{i,j\pm1} - p_{i,j}) \quad (2c)$$

where T is transmissibility defined as follows: $T_{i\pm1/2,j} = k_{i\pm1/2,j}\Delta y/\mu\Delta x$ and $T_{i,j\pm1/2} = k_{i,j\pm1/2}\Delta x/\mu\Delta y$. k is a permeability defined at a the centre of a permeability cell as shown in Figure 1c.

After replacing the fluxes in Equations 2a by the relationships in 2b and 2c, we can derive linear equations involving pressures (Equation 3), which is a 5-point scheme:

$$\begin{aligned}&(T_{i+1/2,j} + T_{i-1/2,j} + T_{i,j+1/2} + T_{i,j-1/2})p_{i,j} - \\ &(T_{i+1/2,j}p_{i+1,j} + T_{i-1/2,j}p_{i-1,j}) - \\ &(T_{i,j+1/2}p_{i,j+1} + T_{i,j-1/2}p_{i,j-1}) = 0\end{aligned} \quad (3)$$

Modification to the transmissibility is accomplished through changing the permeability of relevant cells. On the permeability grid, whenever a cell is cut by one or more faults, its permeability is adjusted. For each cell intersected by one or more faults, DFFM converts each fault intersecting that cell into equivalent fault(s) aligned with each grid canonical direction. An equivalent fault would look like a staircase as shown in Figure 2. For each segment of the staircase, a permeability modification is made for the component of the matrix permeability perpendicular to that segment by calculating a harmonic average of the matrix permeability and the fault permeability along that grid direction. This modification accounts for the fault thickness, the cell scale and permeability. For further details of the DFFM formulation, and the procedure for adjusting permeability, the reader is referred to the paper of Odling *et al.* (2004). Harris *et al.* (2007) apply the 3D version of DFFM to explore the impact of the parameters defining FDZs on the predicted bulk FDZ permeability, connectivity, 'efficiency' as a barrier or retarder to flow, and the 'effective' fault rock throw to thickness relationship for FDZs. Note that similar strategies to incorporate faults into matrix have been developed by other authors (see Manzocchi *et al.* 1998, 1999; Walsh *et al.* 1998*a*, *b*).

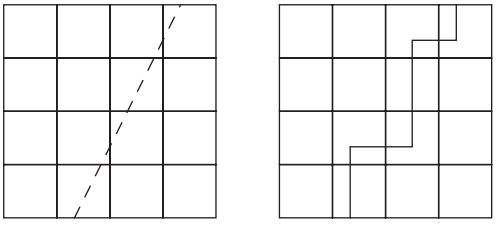

Fig. 2. Illustration of transformation of a fault into a staircase effective fault.

Implicit/explicit discretization of faults and mixed finite-element method

Ma *et al.* (2006) propose a different discretization scheme for FDZ models where fault traces (in 2D) are assumed to be piecewise linear segments. This scheme was adapted from similar schemes for flow modelling in open-fracture systems (e.g. Granet *et al.* 2001; Karimi-Fard & Firoozabadi 2003; Karimi-Fard *et al.* 2003). Given an input fault model, the scheme discretizes the matrix only and represents the faults implicitly by a set of edges of the relevant matrix cells (in an unstructured grid). This approach is referred to as implicit discretization of faults (IDF). An IDF grid, which is a geometrical grid, captures the fault connectivity precisely while utilizing only a fraction of the number of cells that might be required if faults are discretized explicitly and exactly along with the matrix (see Ma *et al.* 2006), another approach which is referred to as the explicit discretization of faults (EDF) method. EDF is used later in this paper to generate a reference solution.

Unlike the schemes for fractured systems, which must model fluid flow both along and across each fracture, the IDF scheme described here neglects the along-fault flow under the assumptions that fault strands have permeability lower than the matrix and are very thin compared to the dimensions of the model domain. To model across-fault flow, the IDF scheme expands each fault segment (cell edge) numerically into a fault parallelogram cell, which closely represents the corresponding original fault segment. The geometrical grid and the fault cells form a computational grid on which the scheme discretizes the flow equations to model both matrix-to-matrix and across-fault flows. The underlying numerical discretization scheme employed is the mixed finite-element method (MFEM) of Raviart & Thomas (1977). MFEM is one of the techniques that possesses two important features required by fluid flow simulation through heterogeneous models, i.e. local mass conservation and flux continuity (see Klausen & Russell 2004 for a review of some those techniques). MFEM has been shown, by numerical experiments, to improve the accuracy of predictions

of the approximate flux within heterogeneous media that have anisotropic and discontinuous permeability distributions (Durlofsky 1994). For simplicity, the scheme used here is labelled as IDF + MFEM. To construct a reference case, where fault strands are explicitly represented in the models, we use a scheme that is labelled as EDF + MFEM. Figure 3 illustrates the IDF approach and the expansion of fault cell-edges. Note that the connecting cells between adjacent fault segments are not required. Figure 4 shows grids generated for a fault model using IDF and EDF using the grid generation package Triangle (Shewchuk 2002).

EDF + MFEM can be implemented following the standard finite-element assembly procedure. To construct a global system of equations for solving both pressure and flux unknowns simultaneously, elementary matrices and right-hand vectors are constructed by MFEM discretization for every cell, and then the contributions of all cells are assembled one by one with respect to both cell facets and cells to form that global system. As shown, IDF + MFEF could be implemented using the same assembly procedure above but excluding the contributions associated with those fault-cell facets that are not common to a matrix cell. In effect, this neglects the along-fault flow. IDF + MFEM is able to achieve higher computational efficiency than EDF + MFEM for dense fault models, though the efficiency may vary according to the fault configuration, the fault-to-matrix permeability contrast, and the flow direction. Note that IDF + MFEM and EDF + MFEM can and have been implemented in both two and three dimensions, although only the implementations for 2D problems are considered in this paper.

The accuracy of IDF + MFEM has been analysed analytically and numerically (Ma *et al.* 2006). Apart from the standard errors due to numerical discretization, there are two additional types of error that arise because of: neglecting the along-fault flow; and expanding the matrix (area or volume) as a result of treating each fault as being composed of zero-thickness linear segments. In terms of the total volumetric flow rate at a model face, the amount of error due to the former is much smaller than, and partly compensates for the overestimate due to, the latter. These two types of error will be small when fault strands are thin and the total volume of the fault-material region is small relative to the model domain. These conditions apply to most cases of interest. Note that EDF + MFEM produces more accurate results than IDF + MFEF does because, unlike the latter, the former represents individual faults exactly and does not introduce additional simplifications in numerical discretization.

Comparison of DFFM and IDF + MFEM

DFFM and IDF + MFEM are based on very different approaches to the discretization of FDZ models. DFFM discretizes the flow equation using a Control-Volume Finite-Difference method on a regular structured grid, and takes into account the flow impacts of the faults by modifying, locally, the matrix permeability of those cells that intersect with one or more of the fault strands. DFFM represents the fault connectivity accurately only if

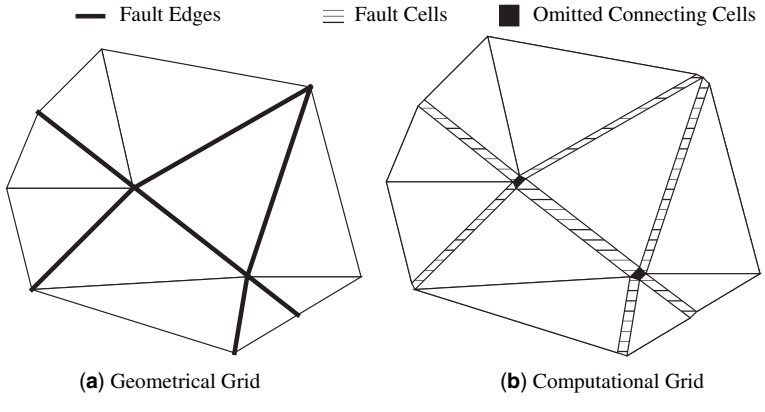

Fig. 3. Illustration of the implicit discretization of faults: (**a**) a geometrical grid for the fault model where the faults form the edges of matrix triangular elements shown in thick lines. (**b**) a computational mesh constructed from the geometrical grid in (a) where the faults have been modelled as rectangular cells (hachured) with omitted 'connecting' cells (black). The rectangular cells are expanded from fault edges numerically rather than physically to approximate the fault segments. From Ma *et al.* (2006).

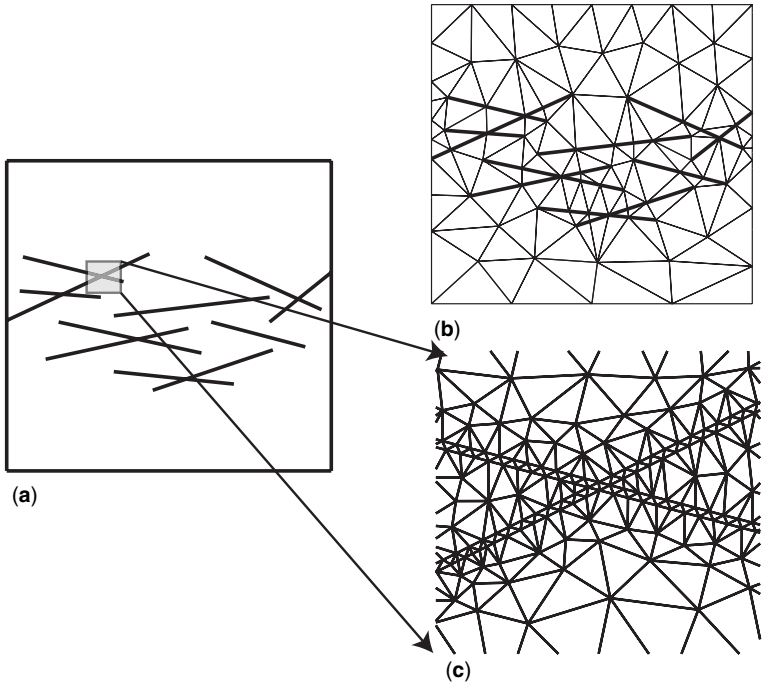

Fig. 4. A fault model and grids generated using IDF and EDF. (**a**) a simple fault model; (**b**) a geometrical grid generated by IDF for the whole model, where faults are shown as thick lines; and (**c**) a part of a grid generated using EDF corresponding to the indicated portion of the fault model in (a). From Ma *et al.* (2006).

the selected regular grid is sufficiently fine (see below). DFFM can only consider a diagonal tensor permeability. On the other hand, IDF + MFEM decomposes a FDZ model, which is assumed to contain (in 2D) piecewise linear fault segments only, into an unstructured grid in which the fault pattern of the model can be represented accurately by the edges of the matrix cells. The method discretizes the flow equations using the MFEM on that grid plus the fault cells that are expanded from the edges of matrix cells that are adjacent to the faults. The MFEM allows full tensor permeability to be specified for the matrix.

Computationally, DFFM generally should be more efficient than IDF + MFEM because it uses a very simple data structure to manage grid and other data and it forms a system of equations for solving pressure unknowns, rather than equations for both pressure and flux unknowns as required by the latter. DFFM domain discretization is trivial even for a FDZ model that contains a large number of faults and this step does not require any special tools. In contrast, IDF relies on special tools to generate unstructured grids, and these tools typically involve intensive computation, especially for FDZ models that contain many faults. However, since IDF represents the fault connectivity accurately for piecewise linear faults, it is possible to generate an unstructured grid that has far fewer cells than a comparable DFFM grid in terms of the accuracy of results calculated on them (see in the next section). Although these issues concerning efficiency may be important in choosing which approach to use in solving a particular problem, our purpose here is not about efficiency. Rather, it is, about examining the way that these approaches can introduce errors.

Application of DFFM and IDF + MFEM to FDZ examples

DFFM and IDF + MFEF are applied to two FDZ models, Model 1 and Model 2 as in Figure 5(a and b) respectively, to allow a numerical comparison of the simulation consequences associated with these two schemes. These two test models are different-sized subregions of a random 2D horizontal slice through a small part of a large-scale 3D fault damage zone model containing on the order of 10^6 fault strands. The full model was generated stochastically using the technique of Harris *et al.* (2003) based on spatial distributional properties derived from two normal faults: the Moab fault in

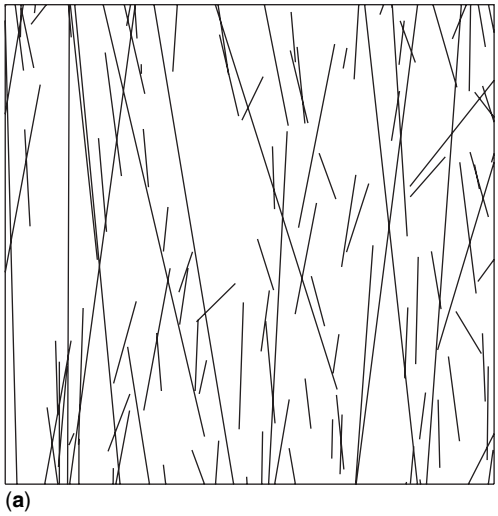

Fig. 5. The two fault models, (**a**) Model 1 and (**b**) Model 2, considered in this paper. An enlarged version of Model 2 is shown in Figure 7a where the intersections among the faults and between them and boundaries can be seen more clearly.

Utah, USA, and the Ninety Fathom fault in NE England (see Harris *et al.* 2003 for details). The selected region corresponds to a part of the fault damage zone with a relatively low density of deformation bands, involving subzones positioned close to the main fault in its footwall block. Models 1 and 2 contain 119 and 19 straight-line fault traces that are 1 mm in thickness (the constant thickness assumption reduces the parameter space for this analysis). The model domains are 10 m × 10 m and 2 m × 2 m, respectively. Each of the models has multiple TGRs in the vertical direction (referring to the coordinates as printed on these pages; 'vertical' is actually horizontal in the original model, and subparallel to the main fault), but no TGRs occur in the horizontal direction of these models, which is roughly perpendicular to the main fault (see Ma & Couples 2007).

The numerical calculations are designed as follows. Using Darcy's law, single-phase steady-state fluid flow is simulated for each model, for horizontal and vertical flow directions (meaning across-fault and along-fault flows), separately, to calculate the upscaled permeability over the model domain. The matrix permeability is assumed to be isotropic, and fixed at 1 millidarcy (mD), whereas the fault permeability is also isotropic but takes on a range of values, namely 10^{-i} mD $\{i = 1, \ldots, 6\}$. The flow boundary conditions are defined as follows. For the vertical flow case, a constant unit pressure gradient (the pressure is in Pascals) is applied from the bottom to the top, with no fluid flow across either side boundary. For the horizontal flow, a constant unit pressure gradient is applied from the left to the right sides, with no fluid flow across either of the bottom and top boundaries. Thus, upscaled permeability in the X and Y directions (strictly speaking, the X and Y components of an upscaled tensor permeability) is calculated separately for each case.

The conditions imposed are in line with those used in local permeability upscaling with simple, pre-defined boundary conditions (see Durlofsky 2003; Pickup *et al.* 2005). If the pre-defined boundary conditions do not coincide with the actual fluid flow regime in the examined model region within its larger context, then these arbitrary conditions can lead to incorrect upscaled fluid flow properties (Christie 1996; Wu *et al.* 2002). Flodin *et al.* (2004) provide a detailed account of this problem in faulted sandstone reservoirs. Upscaling is applicable when the size of the coarse cell is much greater than the effective scale of the heterogeneities within the model. However, this condition may be violated even for faults that are thin and short with respect to the coarse cell scale. This is because the faults can connect to one another and have an effective scale much greater than that of the length of individual fault strands. Recent subgrid simulation techniques may be capable of addressing these issues (Hou & Wu 1997; Arbogast 2002; Chen & Hou 2002; Chen *et al.* 2003; Jenny *et al.* 2003; Aarnes 2004; Ma & Couples 2004). These multi-scale issues are not considered further in this paper since its aim is to compare DFFM and IDF + MFEM numerically.

Domain discretization

Models 1 and 2 are discretized using DFFM, IDF and EDF. Three grid resolutions, 200 × 200, 500 × 500 and 1000 × 1000, are used to generate DFFM grids, denoted with the reference names D200, D500, and D1000. Two IDF grids are generated for each model with the following constraints: the minimum angle in every cell of a grid is 10 degrees, and the maximum area of each cell is less than 1/1000 or 1/30000 of that model domain. The reference names are denoted as I1000 and I30000, respectively. An EDF grid is constructed for both models with the constraints: the minimum angle in every cell of that grid is 10 degrees, and the maximum area is less than 1/30000 of the area of the model. The reference

Table 1. *Statistics of the number cells of the grids used in the numerical comparison. M* and *F indicate the number of matrix cells and the number of fault cells, respectively. For each IDF grid, the number of fault cells is equal to the number of fault edges in that grid*

	E30000		D200	D500	D1000	I1000		I30000	
	M	*F*				*M*	*F*	*M*	*F*
Model 1	595337	287431	40000	250000	1000000	4679	3631	48472	9338
Model 2	71771	18465	40000	250000	1000000	1906	706	46708	2630

name for this model is denoted as E30000. E30000 grids have been verified to contain such a large number of cells that the upscaled permeability values calculated using EDF + MFEM become stable and thus these models provide the best available predictions for the 'true' upscaled permeability of the two fault models. Therefore, the E30000 models are used as references for the results of DFFN and IDF + MFEM below. Table 1 shows the statistics of the number of cells in the generated grids.

Numerical results of upscaling

For both Model 1 and Model 2, and for both the vertical and horizontal flow directions, EDF + MFEM, DFFM and IDF + MFEM were applied, respectively, to generate models to calculate upscaled flow corresponding to the labels E30000, selected D# and I# (where # indicates the grid size as described above). For each fault permeability (i.e. $\boldsymbol{k}_f = 10^{-i}$ mD, $i = 1, \ldots, 6$), the corresponding model upscaled permeability values, denoted as ***KE***, ***KD***# and ***KI***#, are calculated. The results show that:

1) ***KE***, ***KD***# and ***KI***# are in relatively good agreement;
2) ***KD***# and ***KI***# match more closely to ***KE*** with high-resolution grids than they do with low-resolution grids (as expected);
3) both DFFM and IDF + MFEM can over- and under-estimate the upscaled permeability (with errors as large as 10% in some situations with DFFM); and
4) ***KE***, ***KD***# and ***KI***# decrease as the fault permeability decreases, and they 'converge' to a smaller value for the horizontal (across-fault) flow than for the vertical (along-fault) flow, because the fault segments form completely connected barriers/baffles to the horizontal flow but not to the vertical flow (see Fig. 5).

To compare DFFM and IDF + MFEM in detail, the relative errors, $(\boldsymbol{KE} - \boldsymbol{KD}\#)/\boldsymbol{KE}$ and $(\boldsymbol{KE} - \boldsymbol{KI}\#)/\boldsymbol{KE}$, are analysed (i.e. taking the result of EDF + MFEM as the reference). Figure 6a–d shows these relative errors and ***KE*** (red solid lines) as a function of the fault-strand permeability for each of the two models and for each of the two flow directions. Note that DFFM results corresponding to KD200 are also shown in Figure 6d to provide a direct comparison between them and those of KE30000 for that particular case. For horizontal flow (across the fault zone), IDF + MFEM relative errors, $(\boldsymbol{KE} - \boldsymbol{KI1000})/\boldsymbol{KE}$ and $(\boldsymbol{KE} - \boldsymbol{KI30000})/\boldsymbol{KE}$, behave similarly. The relative errors peak around a fault permeability of 0.0001 mD and 0.001 mD for Model 1 and Model 2, respectively, but the errors become smaller at higher and lower fault-to-matrix permeability contrasts. The distribution of the relative errors as a function of fault permeability seems to indicate that, for IDF + MFEM, there is a transition from the faults having little effect on flow (lower permeability contrasts), to the faults forming a significant barrier to flow (higher permeability contrasts). In the transition, it may be necessary to model the fault geometry accurately, or the errors could impact the results. On the other hand, DFFM relative errors, $(\boldsymbol{KE} - \boldsymbol{KD1000})/\boldsymbol{KE}$ for Model 1 and $(\boldsymbol{KE} - \boldsymbol{KD200})/\boldsymbol{KE}$ for Model 2, show a different pattern. Note that D1000 and D200 are at the same grid resolution, taking into account the sizes of the models. The largest absolute errors are less than 7% and 3% for Model 1 and Model 2, respectively. Note that for all models the errors are small for fault permeability greater than 0.001 mD and of little significance in practice. This agrees well with the results of Walsh *et al.* (1998*a*, *b*).

For vertical flow (along the fault zone), the relative errors behave differently from the case for the horizontal flow errors. For IDF + MFEM, the relative errors, especially those of I1000, appear to increase for both models as the fault permeability decreases. Ma *et al.* (2006) argue that this trend may be explained as follows. First, as the fault-strand permeability reduces, the amount of fluid flowing along each fault decreases and could, therefore, compensate less for the primary error (i.e. flow over-estimation) due to the geometrical expansion of the matrix that occurs with the IDF scheme. Second, as the fault-to-matrix permeability contrast

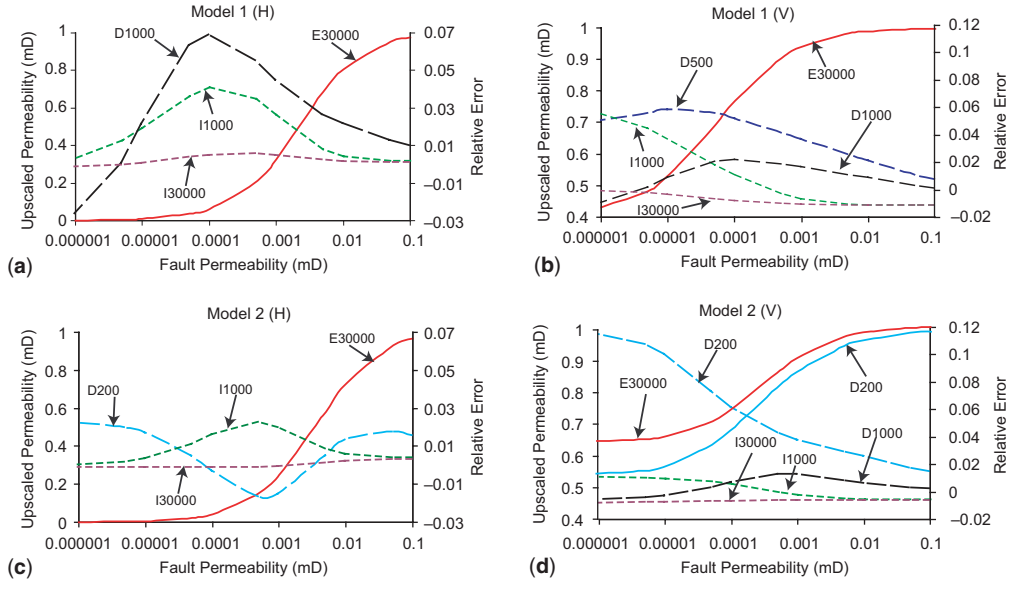

Fig. 6. Upscaled permeability and relative errors for different discretization schemes and resolutions: (**a**) Model 1 for horizontal flow; (**b**) Model 1 for vertical flow; (**c**) Model 2 for horizontal flow; (**d**) Model 2 for vertical flow. The relative error is defined as $(KE - KD|I\#)/KE$, where KE is the upscaled permeability by EDF + MEFE on respective models corresponding to E30000, while $KD|I\#$ is the upscaled permeability by DFFM and IDF + MFEF on respective models corresponding to $D|I\#$ given in Table 1 where # is the number. The KD200 results are also plotted in (d) for a direct comparison with E30000 results. The upscaled permeability results for E30000, and D200 in (d), are shown as solid lines whereas the relative errors are shown as broken lines.

becomes much greater, a larger fraction of the fluid flow must occur in the TGRs between the faults, and finer meshes are required to represent complex structures of faults especially along and inside each TGR. The former is likely to be more important than the latter for sparse fault models, but vice versa for dense fault models. Therefore, for Model 1, as it is a dense model, the increase in the relative errors may reflect a relative inadequacy of discretization inside TGRs when the fault-to-matrix permeability contrast is high. For Model 2, as it is sparse, the monotonic increase in error may be better explained as an artefact of the over-sized matrix. These reasons also seem to explain why the relative errors of IDF + MEFM are more sensitive to the grid resolution for Model 1 than for Model 2 (see the error magnitudes of I1000).

On the other hand, the DFFM errors for Model 1 peak between 0.00001 and 0.0001 mD and $(KE - KD500)/KE$ is less than 6%. For Model 2, there is an apparent inconsistency between $(KE - KD200)/KE$ and $(KE - KD1000)/KE$. $(KE\text{-}KD200)/KE$ increases monotonically to about 12% as the fault permeability decreases, whereas $(KE - KD1000)/KE$, like for Model 1, peaks around 0.001 mD at a maximum of 2%. This inconsistency is investigated (see below) to examine whether the D1000 may resolve additional fault-pattern features that cannot be resolved by the D200. $(KE - KD500)/KE$ is calculated for Model 2, but not shown here and is about 2% smaller than $(KE - KD200)/KE$ at every fault permeability value.

Importance of accurate discretization of TGRs

The fault connectivity of Model 2 is analysed in detail and shows that the D200 grid misrepresents the fault connectivity at two locations. These two locations are marked by the two red boxes in Figure 7a. A zoom-in view of each of them is given at the left column of Figure 7b. At each location, the gap between faults is less than 5 mm and so cannot be resolved with a regular grid of 200 × 200. A regular grid of 1000 × 1000 is sufficient to resolve the gaps. The zoom-in views of equivalent faults corresponding to D200 and D1000 at those locations are shown at the middle column and the right column of Figure 7b, respectively. Further analysis also shows that for this model the D500 grid is not sufficient to resolve the gaps either. This suggests that the two TGRs passing through the two gaps, respectively,

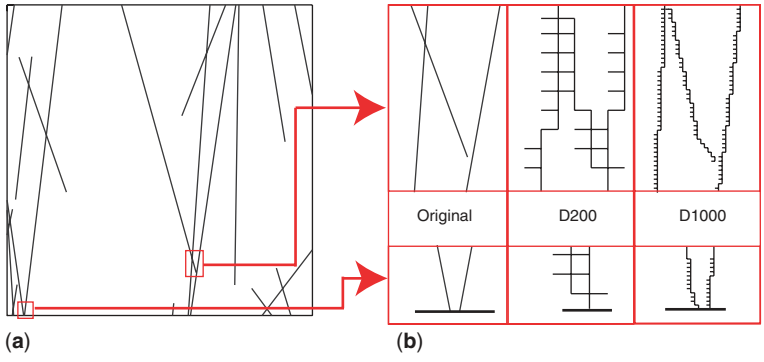

Fig. 7. DFFM discretization for Model 2: (**a**) Model 2 and the two gaps at locations marked by two red boxes; (**b**) zoom-in views of the fault model (left), and the equivalent faults corresponding to D200 (middle) and D1000 (right) at the two locations. There are two TGRs, which pass through the two gaps, respectively, and are mis-discretized into non-TGRs in the D200 (also in D500 not shown here). D1000 is sufficient to resolve these two TGRs. The dark thick lines in the bottom row of (b) indicate segments of the bottom boundary of the model.

influence the fluid flow and are responsible for the increase of the relative errors for Model 2 for the vertical flow.

Summary of numerical comparisons

The numerical output shows that both schemes (i.e. DFFM and IDF + MFEM) can produce reasonably accurate upscaled permeability values in comparison with the reference case (i.e. EDF + MFEM), if there is no TGR in a model or there is no flow-influential TGR being mis-discretized into a non-TGR (as shown for the cases corresponding to Fig. 6a, b and c). However, DFFM may not resolve the gaps between faults when they are smaller than the resolution of the regular grid. In other words, given any particular regular grid, DFFM can misrepresent a TGR as a non-TGR if the model has passages narrower than the resolution of the cells, in which case, DFFM will not be able to account correctly for the fluid flow contribution of that TGR. This is why in the work of Odling *et al.* (2004) an additional procedure was used to determine a fine grid that ensures all gaps between all faults are resolved for a FDZ, though that procedure seems not to be able to determine coarser grids that lead to equally acceptable results with small enough errors.

Unlike DFFM, IDF + MFEM does not suffer from this problem since it represents the fault connectivity accurately. But this is only true for fault models where faults are in the form of piecewise linear segments (or planar faces in 3D). For a model with irregular-shaped faults, the faults may have to be approximated into these simpler forms in order to use standard meshing methods (e.g. Delaunay triangulation) to construct IDF grids. This is particularly true for 3D FDZ models (see Taniguchi & Fillion 1996; Karimi-Fard 2004). The required approximation process could alter the true fault connectivity of a FDZ model, and any resulting discrepancy in the fault connectivity might have significant impacts on the reliability and robustness of simulated flow if some of the alterations occur at critical places. Thus, like DFFM, IDF + MFEM could also suffer from the mis-discretization of TGRs in complex models. Hence, an effective solution to both types of mis-discretization is necessary in practice no matter which scheme is selected when the discretization errors are anticipated to affect the solutions significantly. Researchers performing simulations should recognize that there is a continuing need to appreciate the way that models and their outcome are linked by the choices that must be made within the simulation process. It is not possible to say that any scheme is always safe to use. Clearly a good choice of specific techniques can only be made by taking into account of other factors (e.g. data errors, stochastic model errors) that could affect the uncertainty of outcomes to different degrees.

Using the guiding-grid scheme for accurate domain discretization

Ma & Couples (2007) describe a generic guiding grid scheme that can be used to prevent flow-influential TGRs from being mis-discretized into non-TGRs. This scheme may be applied to FDZ where the flow is likely to take place in TGRs rather than non-TGRs (e.g. high permeability contrast cases). For a given FDZ model, this scheme determines the existence of TGRs and, if they exist,

it identifies a sufficiently fine guiding grid that resolves all flow-influential TGRs. This guiding grid can then be used to guide the construction of regular structured grids (e.g. for approaches like DFFM) or the TGR-preserved linearization of faults prior to the construction of IDF-based unstructured grids (as illustrated here for the case of IDF + MFEM).

This scheme is centred on a Quadtree decomposition. For a model, the Quadtree decomposition partitions each cell recursively into four equal parts (in 2D) if that cell intersects with any fault. This process starts from the whole model, i.e. set to be the initial cell, and records a subdivision level, starting from 0. For any level, TGRs can be identified from connected regions of cells, each of which does not intersect with any fault at a level not greater than the given level. Two properties, the number of TGRs (N_TGRs) and the volume (i.e. area) of TGRs (V_TGRs), can be extracted at each level to provide rough qualitative information on the additional fluid flow contribution due to any emerging TGR.

In order to estimate the flow-influence of TGRs efficiently and directly, a flow-equivalent porous medium 'pipe' can be constructed for each TGR along its skeleton (Ma & Couples 2007). Assembling all of the pipes into a network, and attaching the inlets and outlets, allows the single-phase steady-state flow to be estimated by a low-cost calculation. The changes in the total volumetric flow rate, along with N_TGRs and V_TGRs, as a function of decomposition level, allow us to determine whether a sufficient resolution has been reached. The result of the Quadtree decomposition can easily be converted into a binary image that consists of the matrix pixels (1) and fault pixels (0) (i.e. those cells that contain the matrix only, or otherwise). If the subdivision is terminated at a level of 10 for example, a converted binary image will have a size of $2^{10} \times 2^{10}$ pixels. This binary image can simply be used as a regular grid input for DFFM.

Figure 8 summarizes the adaptive scheme for constructing a guiding grid. An input fault model (Fig. 8a) is decomposed by Quadtree (Fig. 8b) to identify the existence of TGRs and to estimate their geometrical properties (Fig. 8c). Flow networks are constructed to represent each TGR along its skeleton (Fig. 8d), allowing an estimation of its flow influence. The total flow influence of all TGRs (expressed in terms of upscaled permeability

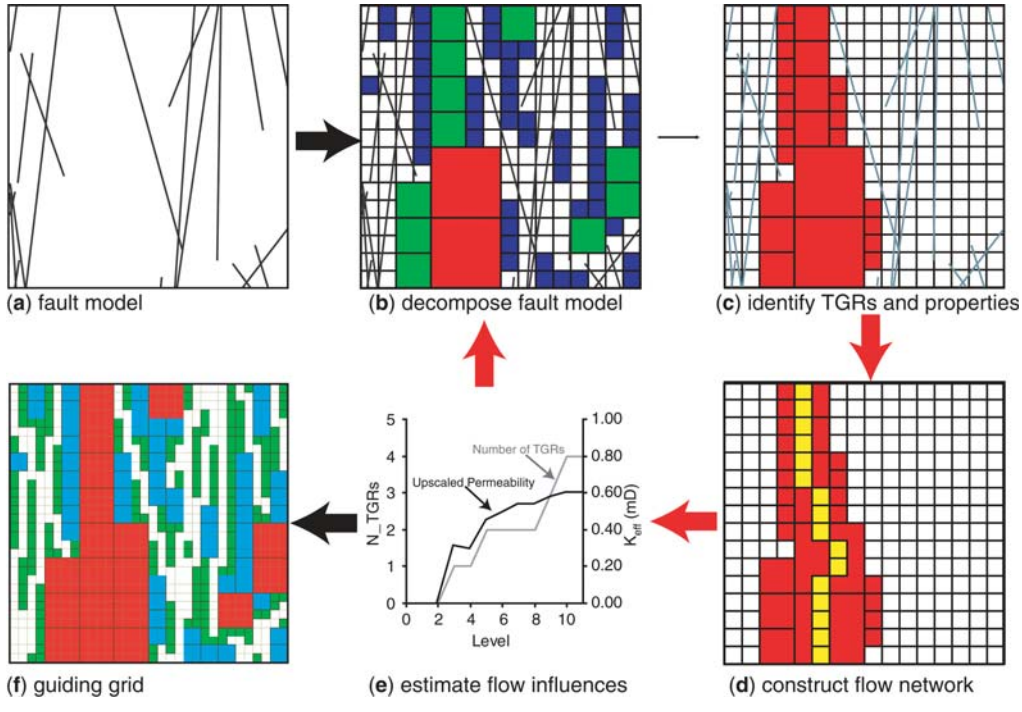

Fig. 8. An adaptive procedure for constructing a guiding grid for a fault model. Cells of different sizes and colours in (**b**) and (**c**) correspond to different decomposition levels. The images shown do not represent the final decomposition, since that produces cells that are too small to distinguish at the scale required to show the whole model in this printed page.

in this case) and TGR geometrical properties are then analysed with respect to the decomposition level (Fig. 8e). Steps (b) to (e) are repeated for the next decomposition level until the increase of each estimate is small. At that decomposition level, the Quadtree is output to construct a guiding grid (Fig. 8f). This scheme could be extended to 3D. Note that a grid determined using this scheme does not necessarily resolve all gaps between faults but only those gaps in corresponding flow-influential TGRs. The reader is referred to the work of Ma & Couples (2007) for more details on this scheme, including its computational efficiency.

Example of guiding grids for DFFM

The guiding-grid scheme was applied to Model 1 and Model 2 to determine appropriate regular grids for DFFM for the vertical flow case only, since there is no TGR in the horizontal direction of these models. For both models, the matrix permeability is set to be 1 mD and the fault is assumed to be impermeable to flow. Figure 9 shows the estimated properties as a function of the subdivision level up to level 11. Data for levels 12 and 13 are not shown because N_TGRs becomes constant and the relative changes of V_TGRs and K_{eff}, from one level to the next, converge after level 10. Note that N_TGRs, V_TGRs and K_{eff} show a non-linear relationship between one and another. Similar non-linear relationships are found by Manzocchi *et al.* (1999) and Walsh *et al.* (1998*a*, *b*) between the proportion of gaps on a fault and its effective permeability. For Model 1 and Model 2, the relative changes of the upscaled permeability are about 10% and 7% due to the emergence of TGRs, i.e. 5th and 6th TGRs for Model 1, and 3rd and 4th TGRs for Model 2, at level 9 and 8, respectively. It has been shown (see Ma & Couples 2007) that the relative change of K_{eff} is a good and robust indicator of additional flow contribution of each newly-emerged TGR when the subdivision level is high. Based on these results, a regular grid comprising $2^{10} \times 2^{10}$ cells (i.e. 1024×1024) should be sufficient to resolve the narrow TGRs. For Model 2, this has been confirmed to be true in the analysis given above.

Remarks on the guiding-grid scheme

In the guiding-grid scheme, the flow influence of each TGR is estimated by calculating the single-phase steady-state flow along the flow network of porous media that have homogeneous and isotropic permeability. This is merely to determine, in an unbiased manner, whether newly-emerged TGRs, i.e. those that are identified as the decomposition progresses, are likely to contribute a significant amount of fluid flow relative to that of existing TGRs. If so, the newly-emerged TGRs should be maintained explicitly in discretization. The actual petro-physical quantities for the systems should be specified at subsequently constructed computational grids. This scheme should be of use, in principle, for multi-phase and multi-component flow too as long as fluid flow takes place predominately in TGRs. Note that this condition can be violated in some fluid flow scenarios as a result of complex interactions between flow mechanisms (e.g. capillary, gravity, etc), differences in flow properties (e.g. fault-to-matrix permeability contrast, phase-mobility, etc) and flow boundary conditions (Manzocchi *et al.* 1998, 1999).

A DFFM regular grid determined using the guiding grid scheme can sometimes contain far more cells than necessary because the grid cells are not aligned with faults. Some of the adjacent rows or columns in that grid could be merged

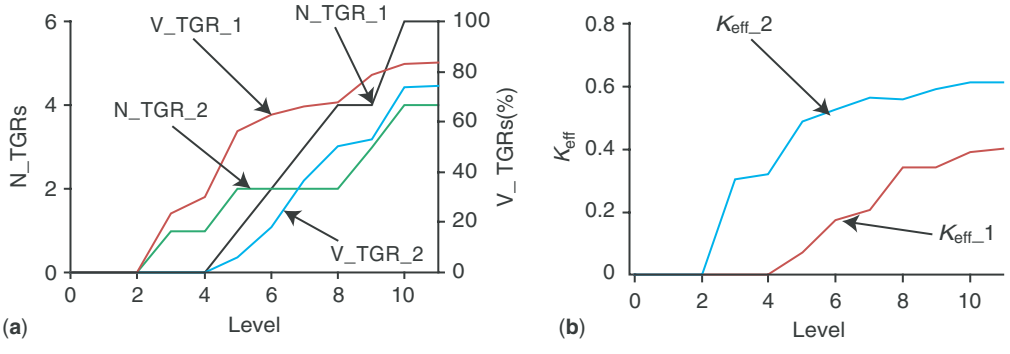

Fig. 9. N_TGRs, V_TGRs and the upscaled permeability, K_{eff}, along the vertical direction as a function of the subdivision level, respectively. Faults are assumed to be impermeable for this suite of models. Note that # indicates the model numbers.

without altering the representations of TGRs. Hence, in practice, the guiding grid scheme might be used in conjunction with a simple post-process to reduce the number of cells.

Discussion

In this paper, we have sought to develop new insights into the factors that can impact the reliability of flow simulation results for heterogeneous systems. The characteristics of fault damage zones make them ideal cases for this purpose. FDZs exhibit extreme property contrasts: in the simplification adopted here, we have only considered a single matrix material type, and a single fault-strand material type, but these materials may have permeabilities that differ by six orders of magnitude or greater. The geometry of FDZs reveals (even in our simplification) that the objects (e.g. the fault strands in our two-component systems) have extreme aspect ratios that demand special approaches in building models and running simulations. The stochastic assembly of large numbers of fault-strand objects (as happens when we create an individual FDZ model) leads to unpredictable variations in the detailed topology of the resulting fault arrays from one realization to the next. Issues related to the connectivity of the fault strands, and how the connectivity is represented during discretization, have been shown to play an important role in governing the bulk system flow behaviour.

One of the comforting outcomes of our work is that we have been able to show that there are multiple numerical approaches (control-volume-finite-difference and mixed-finite-element methods have been examined within this work) that solve the flow equations with a high degree of accuracy when flow-influential TGRs are represented accurately. However, referring to the results presented in this paper we have shown that small changes in the spatial locations of fault strands (i.e. variations in the coordinates describing the end points of the lines representing these elements) can lead to differences (on the order of 10%) in the calculated flow that passes through the whole system (in some flow conditions). Does this outcome have any significance?

The reasons for making permeability predictions are directly linked with economic motivations, commonly involving an estimation of the volumes of fluids that can be extracted from or injected into, a specific subsurface situation, given a set of operating conditions. If the particular subsurface situation involves heterogeneity and complexity, such as a FDZ, then the prediction of fluid flow could vary depending on the modelling/simulation approach that is taken. The prediction is uncertain due to several factors, but one of those factors is the solution error (Christie *et al.* 2005). Our results need to be considered in terms of whether it is possible, based on an understanding of the compatibility of the approach that is selected, relative to the idealized model of the subsurface, to say that the solution error is small or large in comparison with the errors that arise because the model itself is uncertain ('the model errors' in the terminology of Christie *et al.* 2005). Model errors and solution errors can combine in ways that cancel the net error, or they can combine so as to increase the net error. We have demonstrated that these errors can become entangled in practice if one does not examine possible artefacts associated with the discretization methods used.

Our results illustrate that differences in the connectivity (topology in the broad sense) of the fault array can lead to differences in the bulk flow through the system. These effects may be apparent in terms of their impact on fluid flow in one direction, but not in another. Since reality is not known, a model of a fault array may, or may not, be a good representation of that reality. We can say that the details of the model are in error to some extent. The resulting model error (or uncertainty) may be irrelevant in some flow circumstances, but if the flow system changes (this could happen, for example, in an oil reservoir after the drilling of new wells), the model error, or as we have shown here, the way that the model is represented numerically (i.e. the discretization process), may become important considerations.

The analysis described in this paper is not exhaustive. We have identified an issue related to the way that seemingly-minor geometrical variations (either in a model, or in the way that the model is represented during discretization) can result in changes to the flow predictions of a heterogeneous system. We have not developed a set of robust rules that identify the actual scales at which these effects will be manifest in all fault systems. Perhaps that work is worth doing, and the approach based on the identification of TGRs may make that study feasible.

When we create stochastic realizations of FDZs, we must choose a minimum length scale (if we accept that faults occur in power-law distributions; see Harris *et al.* (2003) for a review of these concepts) when we generate each model. Since there is a link between a model and how it is represented numerically, it is not clear how one would decide where to draw the boundary (between faults that are included in the model, and those which are ignored because they are 'too small'). The impracticality of running simulations with smaller and smaller grids means that a multi-scale approach will be required to address this topic.

The analysis described in this paper has reinforced the appreciation of the link between the configuration of a model and the results of simulating flow through that model. We can ask the question: do the 'lessons' revealed in our examination of FDZ upscaling apply equally to cases of large-scale models of faulted reservoirs and their flow simulation? It has become standard practice to represent faults as transmissibility modifiers within a regular grid in reservoir simulators. Using a corner-point style of grid, one can create models that more closely replicate the geometry of fault systems, and there are facilities (such as non-neighbour connections) that permit the user to address many of the issues associated with grid-based models. However, there are potential penalties for adopting some of these methods. For example, corner-point grids may lead to significant numerical errors if the flow is not parallel to the grid coordinates. Fault intersections, and other geometric complexities, may tempt the user to make inappropriate use of the geometric methods that are available in typical finite-difference simulators. Our work highlights the need to give some additional consideration to the interplay between model discretization and the resulting flow simulation.

Conclusions

DFFM and IDF + MFEM have been evaluated to explore their relative merits and weaknesses for 2D FDZ models comprised of arrays of low permeability fault strands. The two schemes employ very different approaches to account for the flow impact of thin faults. DFFM converts fault strands into equivalent fault networks aligned with the canonical directions of a regular grid, and modifies the permeability for those grid cells that intersect with one or more faults using simple averaging schemes. Hence DFFM can handle arbitrary-shaped faults but can only maintain the fault connectivity approximately. On the other hand, by adopting a modified finite element approach, IDF + MFEM represents piecewise linear faults as facets of the elements of a grid to achieve the purpose of maintaining precise fault connectivity. IDF + MFEM makes use of a more accurate scheme than that of DFFM to model intra-matrix and fault-across flow, and allows the full permeability tensor to be specified for the matrix. Computationally, DFFM is simpler than IDF + MFEM as it requires a simple data management internally and does not require any sophisticated and computationally expensive grid-generating tools. A typical DFFM grid can contain more cells than a comparable IDF grid, but the formulation of DFFM results in a less-expensive calculation. The simpler calculation design also means that DFFM can work effectively with models that have many faults.

Both of the schemes work equally well for example 2D models that do not contain TGRs using grids with reasonably low resolutions. For models with TGRs, DFFM is prone to discretization errors due to mis-discretizing TGRs into non-TGRs when the resolution of a selected regular grid is not sufficiently high. This remains true even for linear faults, and the flow contribution resulting from mis-discretized TGRs is not accounted for accurately. The magnitude of the solution error due to such discretization errors depends on the configuration of faults, the fault-to-matrix permeability contrast, and the flow direction. As IDF + MFEM is capable of handling piecewise linear faults only, for models with non-linear faults, a pre-processing would be required to approximate faults into the required form. If this process cannot maintain the fault connectivity of the original fault network, it will also result in similar discretization errors that could become equally significant if they occur at critical places on the flow paths. Hence, both of the schemes can suffer from the same problem of failing to maintain the true fault connectivity, though the problem occurs at different stages in different ways.

The guiding-grid scheme proposed by Ma & Couples (2007) is an effective solution to this problem for DFFM. This scheme can be used to screen for the existence of TGRs for a fault model. Upon identifying the existence of TGRs, it can, at the same time, be used to identify a guiding grid, which resolves flow-influential TGRs. We have shown that such grids can be used effectively to construct suitable DFFM grids.

The comparisons that we have undertaken here highlight the role of topology and how discretization methods can inadvertently mask the flow effects associated with small connections that can occur near the ends of fault strands. If this issue is appropriately acknowledged, then both DFFM and IDF + MFEM represent robust methods for calculating the effective flow properties of FDZs. The scheme for constructing appropriate grids makes it possible to identify important connections, and in future, to quantify and model solution errors induced by geometrical misrepresentations for a more complete set of configurations. The application of commercial reservoir simulation tools to faulted reservoirs has the potential for mis-discretization and the understanding generated here may help in examining these potential effects.

We would like to thank our numerous sponsors who have partially funded this work. Special mention should go to our industrial sponsors Amerada Hess, BG Group, BP,

ConocoPhillips, Kerr KcGee, Shell, Statoil, Total and the Department of Trade and Industry, UK, who supported the BMFFFS Project within the ITF-brokered thematic programme of work on Structurally Complex Reservoirs. We would like to thank the following referees, G. Yielding, T. Taniguchi and J. Walsh, for their comments and suggestions that helped to improve the paper.

References

AARNES, J. E. 2004. On the use of a mixed multiscale finite element method for greater flexibility and increased speed or improved accuracy in reservoir simulation. *Multiscale Modelling and Simulations*, **2**, 421–439.

ARBOGAST, T. 2002. Implementation of Locally Conservative Numerical Subgrid Upscaling Scheme for Two-Phase Darcy Flow. *Computational Geosciences*, **6**, 453–481.

BOURNE, S. & WILLEMSE, E. J. M. 2001. Elastic stress control on the pattern of tensile fracturing around a small fault network at Nash Point, UK. *Journal of Structural Geology*, **23**, 1753–1770.

CAINE, J. S. & FORSTER, C. B. 1999. Fault zone architecture and fluid flow: insights from field data and numerical modelling. *In*: HANEBERG, W. C., MOZLEY, P. S., MOORE, J. C. & GOODWIN, L. B. (eds) *Faults and Subsurface Flow in the Shallow Crust*. AGU Geophysical Monograph, **113**, 101–127.

CHEN, Z. & HOU, T. Y. 2002. A mixed multiscale finite element method for elliptic problems with oscillating coefficients. *Mathematics of Computation*, **72**, 541–576.

CHEN, Y., DURLOFSKY, L. J., GERRITSEN, M. & WEN, X. H. 2003. A coupled local-global upscaling approach for simulating flow in highly heterogeneous formations. *Advances in Water Resources*, **26**, 1041–1060.

CHESTER, F. M. & LOGAN, J. M. 1986. Composition planar fabric of gouge from the Punchbow Fault, California. *Journal of Structural Geology*, **9**, 621–634.

CHRISTIE, M. A. 1996. Upscaling for reservoir simulation. *Journal of Petroleum Technology*, **48**, 1004–1010.

CHRISTIE, M. A., GLIMM, J., GROVE, J. W., HIGDON, D. M., SHARP, D. H. & WOOD-SCHULTZ, M. M. 2005. Error analysis and simulations of complex phenomena. *Los Alamos Science* **29**, 6–25.

COUPLES, D. G. 2005. Seals: the role of geomechanics. *In*: BOULT, P. & KALDI, J. (eds) *Evaluating Fault and Cap Rock Seals*. American Association of Petroleum Geologists, Hedberg Series, 1–22.

COUPLES, G. D., LEWIS, H., OLDEN, P., WORKMAN, G. H. & HIGGS, N. G. 2007. Insights into the faulting process from numerical simulations of rock-layer bending. *In*: LEWIS, H. & COUPLES, G. D. (eds) *The Relationship Between Damage and Localization*. Geological Society, London, Special Publications, **289**, 161–186.

COWIE, P. A. & SCHOLZ, C. H. 1992. Displacement–length scaling relationships for faults: data synthesis and discussion. *Journal of Structural Geology*, **14**, 1149–1156.

DURLOFSKY, L. J. 1994. Accuracy of mixed and control volume finite element approximations to Darcy velocity and related quantities. *Water Resources Research*, **30**, 965–973.

DURLOFSKY, L. J. 2003. Upscaling of geocellular models for reservoir flow simulation: a review of recent progress. *International Forum on Reservoir Simulation*, Buhl/Baden-Baden Germany, June 23–27, 2003.

FLODIN, E. A., DURLOFSKY, L. J. & AYDIN, A. 2004. Upscaled models of flow and transport in faulted sandstone: boundary condition effects and explicit fracture modeling. *Petroleum Geoscience*, **10**, 173–181.

GILLESPIE, P. A., HOWARD, C. B., WALSH, J. J. & WATTERSON, J. 1993. Measurement and characterisation of spatial distributions of fractures. *Tectonophysics*, **226**, 113–141.

GRANET, S., FABRIE, P., LEMONNIER, P. & QUINTARD, M. 2001. A two-phase flow simulation of a fractured reservoir using a new fissure element method. *Journal of Petroleum Science and Engineering*, **32**, 35–52.

HARRIS, S. D., MCALLISTER, E., KNIPE, R. J. & ODLING, N. E. 2003. Predicting the three-dimensional population characteristics of fault zones: a study using stochastic models. *Journal of Structural Geology*, **25**, 1281–1299.

HARRIS, D. S., VAZSI, A. & KNIPE, R. J. 2007. Three-dimensional upscaling of fault damage zones for reservoir simulation. *In*: JOLLEY, S. J., BARR, D., WALSH, J. J. & KNIPE, R. J. (eds) *Structurally Complex Reservoirs*. Geological Society, London, Special Publications, **292**, 353–374.

HOU, T. Y. & WU, X. H. 1997. A multiscale finite element method for elliptic problems in composite materials and porous media. *Journal of Computational Physics*, **131**, 169–189.

JENNY, P., LEE, S. H. & TCHELEPI, H. A. 2003. Multi-scale finite-volume method for elliptic problems in subsurface flow simulation. *Journal of Computational Physics*, **187**, 47–67.

JOURDE, H., FLODIN, E. A., AYDIN, A., DURLOFSKY, L. & WEN, X. 2002. Computing permeability of fault zones in eolian sandstone from outcrop measurements. *American Association of Petroleum Geologists Bulletin*, **86**, 1187–1200.

KARIMI-FARD, M. 2004. Growing Region Techniques Applied to Grid Generation of Complex Fractured Porous Media. *Proceedings of the 9th European Conference on the Mathematics of Oil Recovery B007*, Cannes, France, 30 August–2 September 2004, A038.

KARIMI-FARD, M. & FIROOZABADI, A. 2003. Numerical simulation of water injection in 2D fractured media using discrete-fracture model. *SPE Reservoir Evaluation & Engineers*, **6**, 117–126.

KARIMI-FARD, M., DURLOFSKY, L. J. & AZIZ, K. 2003. An efficient discrete fracture model applicable for general purpose reservoir simulators. *SPE* 79699.

KLAUSEN, R. & RUSSELL, T. 2004. Relationships among some locally conservative discretization methods which handle discontinuous coefficients. *Computational Geosciences*, **8**, 341–377.

KNIPE, R. J., JONES, G. & FISHER, Q. J. 1998. Faulting, fault seal and fluid flow in hydrocarbon reservoirs: an introduction. *In*: JONES, G., FISHER, Q. J. & KNIPE, R. J. (eds) *Faulting, Fault Sealing and Fluid Flow in Hydrocarbon Reservoirs*. Geological Society, London, Special Publications, **147**, vii–xxi.

LEWIS, H., COUPLES, G. D., OLDEN, P., HALL, S. A. & MA, J. 2004. Geomechanical Models of Fault Zones – Complex Behavior in Simple Fault Zones and the Consequences. Euro-Conference 2004 on Rock Physics and Geomechanics, GeoForschungsZentrum Potsdam, Germany, 20–23 September 2004.

LEWIS, H., HALL, S. A., GUEST, J. & COUPLES, G. D. 2007. Kinematically-equivalent but geomechanically-different simulations of fault evolution: the role of loading configurations. *In*: JOLLEY, S. J., BARR, D., WALSH, J. J. & KNIPE, R. J. (eds) *Structurally Complex Reservoirs*. Geological Society, London, Special Publications, **292**, 159–172.

MA, J. & COUPLES, G. D. 2004. A finite element upscaling technique based on the heterogeneous multiscale method. *Proceedings of the 9th European Conference on the Mathematics of Oil Recovery B007*, Cannes, France, 30 August–2 September 2004.

MA, J. & COUPLES, G. D. 2007. Construction of guiding grids for flow modelling in fault damage zones with through-going regions of connected matrix. *Computer & Geosciences*, **33**, 411–422; doi:10.1016/j.cageo.2006.06.004.

MA, J., COUPLES, G. D. & HARRIS, S. D. 2006. A mixed finite-element technique based on implicit discretization of faults for permeability upscaling in fault damage zones. *Water Resources Research*, **42**, W08413.

MAERTEN, L., GILLESPIE, P. & DANIEL, J.-M. 2006. Three-dimensional geomechanical modeling for constraint of subseismic fault simulation. *American Association of Petroleum Geologists Bulletin*, **90**, 1337–1358.

MANZOCCHI, T., RINGROSE, P. S. & UNDERHILL, J. R. 1998 Flow through fault systems in high-porosity sandstone. *In*: COWARD, M. P., DALTABAN, T. S. & JOHNSON, H. (eds) *Structural Geology in Reservoir Characterization*, Geological Society, London, Special Publications, **127**, 65–82.

MANZOCCHI, T., WALSH, J. J., NELL, P. A. R. & YIELDING, G. 1999. Fault transmissibility multipliers for flow simulation models. *Petroleum Geoscience*, **5**, 53–63.

ODLING, N. E., HARRIS, S. D. & KNIPE, R. J. 2004. Permeability scaling properties of fault damage zones in siliclastic rocks. *Journal of Structural Geology*, **26**, 1727–1747.

PICKUP, G. E., STEPHEN, K. D., MA, J., ZHANG, P. & CLARK, J. D. 2005. Multi-stage Upscaling: Selection of Suitable Methods. *Transport in Porous Media*, **581–2**, 191–216; doi: 10.1007/s11242-004-5501-5.

RAVIART, R. A. & THOMAS, J. M. 1977. A mixed finite element method for 2nd order elliptic problems. *In*: GALLIGANI, I. & MAGGNES, E. (eds) *Mathematical Aspects of the Finite Element Method*, Lecture Notes in Mathematics 606, Springer-Verlag, New York, 292–315.

SCHOPFER, M. P. J., CHILDS, C. & WALSH, J. J. 2006. Localisation of normal faults in multilayer sequences. *Journal of Structural Geology*, **28**, 816–833.

SHEWCHUK, J. R. 2002. Delaunay refinement algorithms for triangular mesh generation. *Computational Geometry: Theory and Applications*, **221–3**, 21–74.

SHIPTON, Z. K. & COWIE, P. A. 2001. Damage zone and slip-surface evolution over mm to km scales in high-porosity Navajo sandstone, Utah. *Journal of Structural Geology*, **23**, 1825–1844.

TANIGUCHI, T. & FILLION, E. 1996. Numerical experiments for 3-dimensional flow analysis in a fractured rock with porous matrix. *Advances in Water Resources*, **19**, 97–107.

VASZI, A. Z., HARRIS, S. D. & KNIPE, R. J. 2004. 3D upscaling of fault damage zones for reservoir modelling. *9th European Conference on the Mathematics of Oil Recovery*, 30 August–2 Sept. 2004, Cannes, France.

WALSH, J. J., WATTERSON, J., HEATH, A., GILLESPIE, P. A. & CHILDS, C. 1998*a*. Assessment of the effects of subseismic faults on bulk permeabilities of reservoir sequences. *In*: COWARD, M. P., DALTABAN, T. S. & JOHNSON, H. (eds) *Structural Geology in Reservoir Characterization*, Geological Society, London, Special Publication, **127**, 99–114.

WALSH, J. J., WATTERSON, J., HEATH, A. E. & CHILDS, C. 1998*b*. Representation and scaling of faults in fluid flow models. *Petroleum Geoscience*, **4**, 241–251.

WU, X. H., EFENDIEV, Y. & HOU, T. Y. 2002. Analysis of upscaling absolute permeability. *Discrete and Continuous Dynamical Systems*, Series **B 2**, 185–204.